

Molecular Assembly of Manganese Fluorinated Mesoporphyrin Monolayer on a Gold Electrode

Taku Yamada, Seiji Kikushima,[†] Takami Hikita,[†] Akishi Nara,^{††} Etuo Nishio,^{††} Toshiaki Ohtsuka, and Mamoru Nango*[†]

Division of Molecular Chemistry, Graduate School of Engineering, Hokkaido University, Sapporo 060-8628

[†]Department of Applied Chemistry, Nagoya Institute of Technology, Gokiso-cho, Showa-ku, Nagoya 466-8555

^{††}Nicolet Japan Co., 2-4-1, Terauchi, Toyonaka, Osaka 560-0872

(Received March 9, 2000; CL-000233)

Disulfide-linked manganese mesoporphyrin derivatives separated by spacer methylene groups (Figure 1) were synthesized and then the porphyrin derivatives were assembled on a gold electrode. Cyclic voltammetry (CV) of the porphyrin monolayer on a gold electrode showed that one set of waves was clearly visible, corresponding to the consecutive mono-electronic reduction of the manganese porphyrin unit, depending upon the spacer methylene groups. Interestingly, a large positive-shift of the redox potential for the mesoporphyrin was observed due to fluorination of the porphyrin ring.

Porphyrin pigments play an important role in electron-transfer reactions of biological processes such as photosynthesis.¹ Synthetic porphyrin models can be very helpful in studying the effects of the structure of porphyrins and the distance between porphyrins in electron transfers of biological processes.² Recently, electron transfer in a self-assembled monolayer (SAM) of tetraphenylporphyrin derivative on a gold electrode is reported to clarify the electron transfer on the surface of the electrode.³ It is interesting to note that SAM of porphyrin derivative on a gold electrode can easily examine the effect of the distance on the electron-transfer rate by controlling the distance between the electrode and porphyrin.^{3f} We now report the synthesis of disulfide-linked manganese mesoporphyrin (MnMP-C₁₂-S)₂ and its fluorinated mesoporphyrin derivative (MnMPF₄-C₁₂-S)₂ (Figure 1) and then, characterize the effect of the structure of porphyrins on electron transfer in the self-assembled porphyrin monolayer on a gold electrode. We reasoned that the fluorinated mesoporphyrin was used because the electron transfer of mesoporphyrin on electrode modified with lipid bilayers was more efficiency than tetraphenylporphyrin^{2b} and also an enhanced electron transfer across a liposomal membrane was observed due to the fluorination of the porphyrin.^{2a}

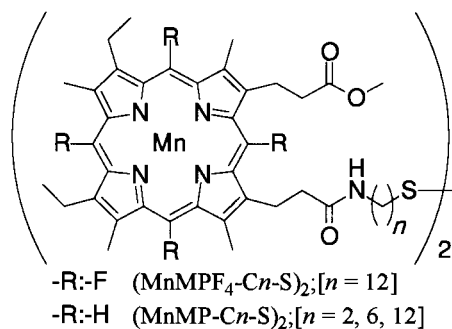


Figure 1. Structure of manganese porphyrin derivatives.

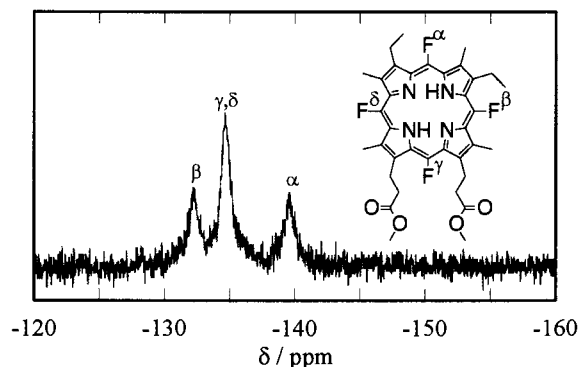


Figure 2. ¹⁹F NMR spectrum of MPF₄DME in CDCl₃.

Mesoporphyrin IX dimethyl ester (MPDME) was fluorinated by using *N*-fluoro-2,3,4,5,6,-pentachloropyridinium triflate (FP-T 1100, Onoda) with hexafluorobenzene/acetonitrile (20/1) and purified by HPLC with acetone/methanol/water (74/20/6), resulting in fluorinated mesoporphyrin IX dimethyl ester (MPF₄DME) in 9.3% yield.⁴ ¹⁹F NMR spectrum of MPF₄DME in CDCl₃ solution substantiated the assigned structure as shown in Figure 2.⁵ Mesoporphyrin IX methyl ester (MPMME) and its fluorinated compound (MPF₄MME) were synthesized by the hydrolysis of MPDME or MPF₄DME in 6 M HCl. The coupling reaction between MPMME or MPF₄MME and bis(12-aminododecyl)disulfide using ethyl chloroformate gave disulfide-linked mesoporphyrin (MP-C₁₂-S)₂ or its fluorinated derivative (MPF₄-C₁₂-S)₂, respectively. Preparation of the manganese complex was carried out by treatment of disulfide-linked free-base mesoporphyrin derivatives with manganese acetate in acetic acid. ¹H NMR, ¹⁹F NMR, FAB-MS and UV/Vis. spectra of porphyrin derivatives support unambiguously the assigned structure.⁶

The porphyrin monolayers on a gold electrode were formed by immersing a gold-coated substrate into a chloroform solution containing disulfide-linked manganese mesoporphyrin derivatives, followed by sufficient rinsing with chloroform. SAM of porphyrin derivatives on a gold electrode was studied with infrared reflection-absorption spectroscopy (IR-RAS), X-ray photoelectron spectroscopy (XPS) and UV/Vis. spectra. IR-RAS measurement showed characteristic absorption of the methylene group^{3e,7} and XPS signals (Table 1), indicating elements of the porphyrin derivative on the gold electrode.^{3b,c,e,8} The S(2p_{3/2}) energies are in good agreement with the reported values for thiolate bound to gold. Furthermore, visible absorption spectra of MnMP-C₁₂-S or MnMPF₄-C₁₂-S monolayer on a gold membrane exhibited the characteristic absorption of the porphyrin ring. For example, the absorption maximum length

Table 1. Binding energy (eV) of manganese mesoporphyrin monolayers on a gold electrode^a

	C(1s)	N(1s)	O(1s)	F(1s)	S(2p _{3/2})
MnMPF ₄ -C ₁₂ -S	284.8	399.8	532.2	690.0	161.6
MnMP-C ₁₂ -S	285.0	399.9	532.4	— ^b	162.0

^a The X-ray source was a monochromatic Al K α . The pass energy was 20 eV. ^bNot applicable.

(λ_{\max} : 458 nm) of MnMP-C₁₂-S monolayer on a gold membrane in dimethyl sulfoxide (DMSO) solution nearly equaled that of MnMPDME (λ_{\max} : 455 nm) in DMSO solution. The area of one molecule (molecular size: $3.3 \times 1.3 \times 0.3 \text{ nm}^3$) on the gold electrode is determined to be 1.3 nm^2 assuming that the porphyrin inclines to the gold surface. In 0.1 M phosphate buffer (pH 7.0) solution, the Soret band was broadened and red-shifted relative to the corresponding spectra in DMSO solution and to those of mesoporphyrin derivatives on the gold electrode.^{3a,d,e} The red-shift is probably due to strong interaction among the porphyrins on a gold surface.

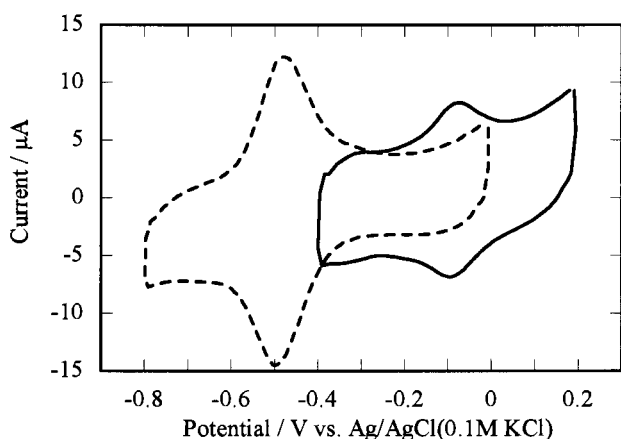


Figure 3. Cyclic voltammograms of MnMPF₄-C₁₂-S (solid line) and MnMP-C₁₂-S (dashed line) monolayer on the gold electrode in DMSO containing 0.1 M TBAP: scan rate 0.3 V/s, electrode area 1.0 cm^2 .

Alternatively, the effect of fluorination of porphyrin on electron transfer in a self-assembled porphyrin monolayer on a gold electrode was examined by CV. Figure 3 shows cyclic voltammograms of MnMPF₄-C₁₂-S and MnMP-C₁₂-S monolayers on a gold electrode in DMSO solution containing 0.1 M tetrabutylammonium perchlorate (TBAP). One set of waves in each was clearly visible, corresponding to the consecutive mono-electronic reduction of the manganese porphyrin unit Mn(III)/Mn(II). The peak current of MnMP-C_n-S monolayers depended on the spacer methylene length, where the largest current was observed when $n = 12$. The electron-transfer rate constant of MnMP-C_n-S [$n = 2, 6, 12$] monolayers was estimated by using Laviron's equation,⁹ in which the rate increased with an increase in the spacer methylene-chain length ($C_2 = 75 \text{ s}^{-1}$, $C_6 = 90 \text{ s}^{-1}$, $C_{12} = 115 \text{ s}^{-1}$). Furthermore, the redox potential of MnMPF₄-C₁₂-S (ΔE° : -0.09 V vs. Ag/AgCl (0.1 M KCl)) or MnMP-C₁₂-S (ΔE° : -0.49 V) monolayers on a gold electrode in

DMSO nearly equaled that of MnMPF₄DME (ΔE° : -0.08 V) or MnMPDME (ΔE° : -0.48 V) in DMSO solution containing 0.1 M TBAP, respectively. Interestingly, the redox potential of the MnMPF₄-C₁₂-S monolayer (ΔE° : -0.09 V) on a gold electrode was largely positive-shifted by 0.40 V due to fluorination of the porphyrin ring. It is interesting to note that the fluorination of the mesoporphyrin ring clearly changes the redox potential of the porphyrin on the electrode so that the electron transfer of the mesoporphyrin monolayer in buffer solution may be observed by minimizing the influence of the hydrogen-evolution on the electrode.

The present work was partially supported by a Grant-in-Aid from the Ministry of Education, Science, Sports, and Culture, Japan.

References and Notes

- a) W. A. Cramer and D. B. Knaff, in "Energy Transduction in Biological Membranes," Springer-Verlag, New York (1991). b) "Chlorophylls," ed. by H. Scheer, CRC Press, Florida (1991).
- a) K. Iida, M. Nango, M. Matsuura, M. Yamaguchi, K. Sato, K. Tanaka, K. Akimoto, K. Yamashita, K. Tsuda, and Y. Kurono, *Langmuir*, **12**, 450 (1996). b) M. Nango, T. Hikita, T. Nakano, T. Yamada, M. Nagata, Y. Kurono, and T. Ohtsuka, *Langmuir*, **14**, 407 (1998).
- a) J. Zak, H. Yuan, M. Ho, L. K. Woo, and M. D. Porter, *Langmuir*, **9**, 2772 (1993). b) J. E. Hutchison, T. A. Postletmwaite, and R. W. Murray, *Langmuir*, **9**, 3277 (1993). c) T. Akiyama, H. Imahori, and Y. Sakata, *Chem. Lett.*, **1994**, 1447. d) T. A. Postletmwaite, J. E. Hutchison, K. W. Hathcock, and R. W. Murray, *Langmuir*, **11**, 4109 (1995). e) K. Shimazu, M. Takechi, H. Fujii, M. Suzuki, H. Saiki, T. Yoshimura, and K. Uosaki, *Thin Solid Films*, **273**, 250 (1996). f) H. Imahori, H. Norieda, S. Ozawa, K. Ushida, H. Yamada, T. Azuma, K. Tamaki, and Y. Sakata, *Langmuir*, **14**, 5335 (1998).
- Y. Naruta, F. Tani, and K. Maruyama, *Tetrahedron Lett.*, **33**, 1069 (1992).
- T. R. Janson, and J. J. Katz, *J. Magn. Reson.*, **6**, 209 (1972).
- a) MPF₄DME. ¹H NMR(CDCl₃): δ -6.4(2H, s, pyrrole-NH), 1.6(6H, t, Ar-CH₂CH₃), 3.0(4H, m, Ar-CH₂CH₂COOCH₃), 3.3(12H, m, Ar-CH₃), 3.7(6H, m, Ar-CH₂CH₂COOCH₃), 3.8(4H, m, Ar-CH₂CH₃), 4.1(4H, m, Ar-CH₂CH₂COOCH₃). MS(FAB): m/z 666 (M⁺). UV/Vis. (CHCl₃): λ_{\max} 400 nm (ϵ 183 $\text{mM}^{-1} \text{ cm}^{-1}$), 465(2.4), 498(12.0), 531(3.4), 586(2.6), 642(5.0). b) (MPF₄-C₁₂-S)₂. ¹H NMR (CDCl₃): δ -5.1(4H, s, pyrrole-NH), 1.3(40H, m, NCH₂(CH₂)₁₀CH₂S), 1.7(12H, t, ArCH₂CH₃), 2.7(4H, m, NCH₂(CH₂)₁₀CH₂S), 3.1(8H, m, Ar-CH₂CH₂-COOCH₃), 3.2(4H, m, NCH₂(CH₂)₁₀CH₂S), 3.5(24H, m, Ar-CH₃), 3.7(6H, m, Ar-CH₂CH₂COOCH₃), 3.9(8H, m, Ar-CH₂CH₃), 4.2(8H, m, Ar-CH₂CH₂COOCH₃), 5.3(2H, m, NHCH₂). MS(FAB): m/z 1702 (M⁺). UV/Vis. (CHCl₃): λ_{\max} 399 nm, 467, 500, 531, 586, 642. c) (MnMPF₄-C₁₂-S)₂. MS(FAB): m/z 1806(MH⁺). UV/Vis. (CHCl₃): λ_{\max} 473 nm, 572, 609. d) (MnMP-C₂-S)₂. MS(FAB): m/z 1383(MH⁺). UV/Vis. (CHCl₃): λ_{\max} 460 nm, 548. e) (MnMP-C₆-S)₂. MS(FAB): m/z 1495(MH⁺). UV/Vis. (CHCl₃): λ_{\max} 459 nm, 549. f) (MnMP-C₁₂-S)₂. MS(FAB): m/z 1663(MH⁺). UV/Vis. (CHCl₃): λ_{\max} 460 nm, 549.
- M. D. Porter, T. B. Bright, D. L. Allara, and C. E. D. Chidsey, *J. Am. Chem. Soc.*, **109**, 3559 (1987).
- R. G. Nuzzo, B. R. Zegarski, and L. H. Dubois, *J. Am. Chem. Soc.*, **109**, 733 (1987).
- E. Laviron, *J. Electroanal. Chem.*, **101**, 19 (1979).